320674-1-F

INVESTIGATION OF AUDIO DEGRADATION IN AUTOMOTIVE RADIO SYSTEMS

by

Donald F. Herrick
The University of Michigan
Radiation Laboratory
Ann Arbor, Michigan 48109

Final Report

15 December 1976 - 15 June 1977

June 1977

Purchase Order No. 47-J-552504-GM

Prepared for

Electrical and Electronics Division
Ford Motor Company
Dearborn, Michigan 48121

ABSTRACT

Vehicle related sources of radio interference and their coupling mechanisms were investigated. The vehicle ignition system and instrument voltage regulator were found to be the primary sources of interference, with the former being more dominant. Both sources generate radiated fields which are coupled to the vehicle antenna. The resultant audio noise was analyzed and a test instrument constructed to measure the noise level in terms of the average peak-to-peak amplitude of the noise voltage impulses at the radio speaker terminals. The test instrument has been delivered to Ford Motor Company for evaluation and correlation with their subjective criteria for evaluating radio performance. Methods for predicting radio interference from vehicle radiation measurements such as those specified by the Society of Automotive Engineers Standard SAE J551c were examined and found to be inappropriate.

TABLE OF CONTENTS

1. INTRODUCTION

It is well known that spark ignition systems and other electrical equipment in motor vehicles are potential sources of radio frequency interference (RFI) which may ultimately lead to audio degradation in vehicle-installed radio sets. At the present time, the level of audio degradation and its acceptability are being judged on an entirely subjective basis. This subjective evaluation is strongly influenced by audio program content, broadcast signal strength and the perceptions of the individual listener; and the test results are often inconsistent. Improved measurement techniques are therefore required. In addition, a greater knowledge of the levels of radiation generated by individual vehicle components and their effects on radio performance is also required to maintain compatability of the radio set with the vehicle.

The present investigation has been directed toward radio interference in the commercial FM broadcast band which is attributable to the operation of the vehicle in which the radio is installed. The results and conclusions presented in the following report are based on test data obtained from two 1977 Mercury Cougars, test vehicle identification numbers 526 T 129 and 526 T 130, supplied by the Ford Motor Company. These vehicles were identical from a manufacturing standpoint, i.e. same make, model and accessories. Both vehicles had eight cylinder engines and were equipped with an Aeroneutronic AM/FM stereo radio with an eight track tape player. Standard test conditions for the radios were first established and measurements then made to determine the dominant RFI sources and their coupling mechanisms. The results are given in Section 2. Analysis of the audio noise produced by these sources and the development of objective interference measurement techniques are presented in Sections 3 and 4. The applicability of methods for predicting radio interference based on vehicle radiation measurements is also discussed.

2. INVESTIGATION OF RFI SOURCES

The primary objectives of this part of the investigation were to locate those vehicle components which produce audible noise in the radio and determine the mechanism by which radio interference occurs. In order to obtain consistent results throughout the investigation it was first necessary to establish some standard test conditions.

2.1 Standard Test Conditions

The RF signal strength, radio control settings and vehicle engine operating conditions represent variables which strongly effect the level of vehicle related radio interference. With respect to the level of the RF signal at the radio antenna terminals, initial observations indicate that maximum interference is obtained when the radio is tuned to a "weak" RF carrier, whereas no interference is detectable above the thermal noise of the radio in the presence of a "strong" RF carrier or when the radio is detuned (absence of an RF carrier). A controlled RF carrier is therefore necessary when making interference measurements, and since commercial broadcast signals are not suitable for this purpose, the required signal was generated using laboratory equipment. The standard model for the vehicle antenna used by Ford Motor Company assumes an impedance of 100 Ω, and the RF signal sources used throughout the investigation were therefore designed so as to be representable by a voltage source having an internal impedance of 100 Ω. A "weak" RF carrier was simulated by adjusting the source output to obtain an RMS voltage of 30 μV across a matched load. This is slightly greater than the threshold (approximately 10 μV) required to maintain automatic gain control (AGC) of the RF amplifier stage of the radio. The following procedure was used to set the radio controls:

A. Set the radio tone control to full treble and the fader control to full front. (Radios having a balance control should be adjusted for equal output on each channel).

B. Set the RF source to the desired test frequency and adjust the output level to obtain an RMS voltage of 30 μV across a 100 Ω load.

C. Connect the source to the radio antenna terminals and modulate the RF carrier with a 400 Hz tone at 35 KHz deviation. With the volume control fixed, tune the radio to the carrier by maximizing the output at the speaker terminals.

D. Adjust the volume control to obtain a peak-to-peak voltage of 1.5 V at the speaker terminals.

The above procedure establishes a repeatable set of test conditions for the radio, henceforth referred to in this report as "standard test conditions". Unless otherwise noted, all measurements were made under standard test conditions with the vehicle stationary and the engine operating at 1000 RPM under no load, i.e. with the transmission in a neutral gear. It should be noted that the effects of engine speed and load on the level of radio interference were not studied as a part of the present investigation and the values stated were chosen rather arbitrarily as a convenient reference.

The audio noise in the radio output was observed by connecting an oscilloscope across the right (passenger side) front speaker terminals. Since one speaker terminal is a signal ground, proper polarity must be observed when connecting the oscilloscope or other test equipment. Measurements were made for both modulated and unmodulated carriers. Although modulation by either a single tone or an audio program may effect subjective evaluations of the audio noise, it was found that there was no difference in the noise voltage waveform between the modulated and unmodulated cases. However, the presentation and analysis of these waveforms is much easier in the absence of the modulating signal, and the data presented are therefore limited to this case.

2.2 Interference Sources and Their Coupling Mechanisms

As shown in Figure 1, the coupling of interference signals to the radio set may be attributed to one or more of the following mechanisms: (1) penetration of the radio chassis by electromagnetic fields, (2) radiative coupling to the speaker cables, (3) power line conducted interference and (4) radiative coupling to the vehicle antenna. Tests were performed to evaluate separately the amount of interference introduced by each of these coupling mechanisms.

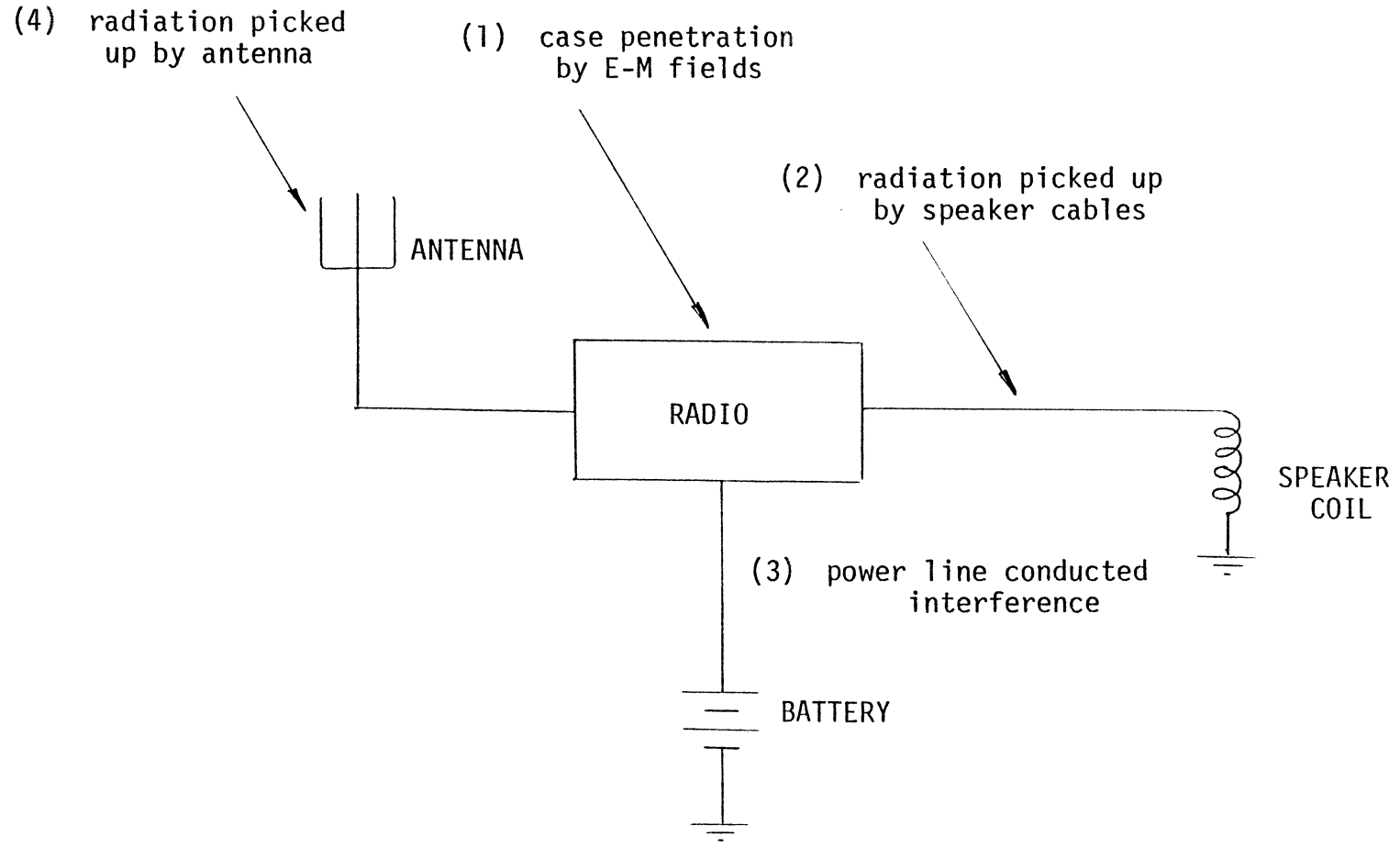

Figure 1. Interference mechanisms in vehicle-installed radios

Since case penetration cannot be measured directly, the radio set was isolated from the vehicle electrical system and the interference produced by mechanisms other than case penetration was minimized. The radio was powered by an auxilliary automotive battery, the speakers were replaced by 3.2 Ω resistive loads, and the RF carrier was simulated by directly coupling the output of an FM signal generator to the radio antenna terminals. All components were located in close proximity to the radio and the length of electrical leads was kept to a minimum. The test set-up is shown in Figure 2. The resistive matching network inserted between the signal generator and the radio antenna terminals was recommended (and supplied) by Ford Motor Company for the purpose of simulating the antenna impedance. With the radio set to standard test conditions, no interference was observed due to operation of the vehicle engine. The resistive loads were removed and the speaker system reconnected in its production configuration. Again, there was no observable interference. Hence, neither case penetration nor radiative coupling to the speaker cables contribute to radio interference.

To evaluate the level of power line conducted interference, the radio power supply was restored to its production configuration. A photograph of the oscilloscope display while the engine was operating is shown in Figure 3. The upper trace shows the actual interference signal on the positive supply line and the lower trace is the resultant noise produced at the speaker terminals. Both signals have a period of approximately 15 ms. This corresponds to the time between ignition events at an engine speed of 1000 RPM and thus indicates that the vehicle ignition system is the source of the interference. Varying the engine speed changes the period of the noise signal proportionally. It is remarked that although the electrical noise signal at the speaker terminals was measurable, no audible noise was perceived when listening to the radio.

The last interference mechanism to be considered is radiative coupling to the vehicle antenna. The test set-up used for this purpose is shown in Figure 4. In this case, the vehicle antenna was used as the signal source and the RF carrier was radiated from a half-wavelength resonant dipole antenna fed by an FM signal generator. The radio and signal generator were tuned to an unoccupied frequency in the FM band and the level of the carrier was set by connecting the vehicle antenna to a spectrum analyzer as indicated in Figure 5.

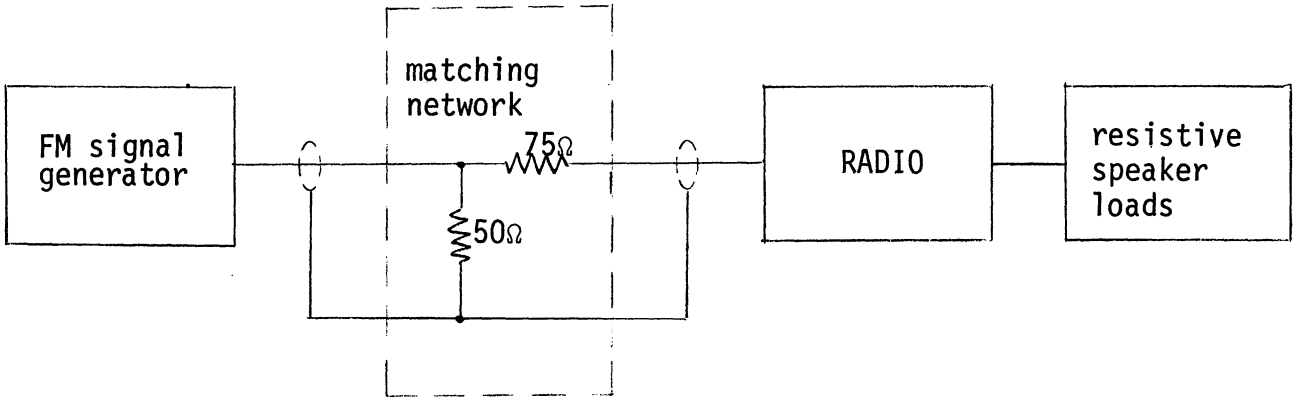

Figure 2. Test set-up for evaluating case penetration

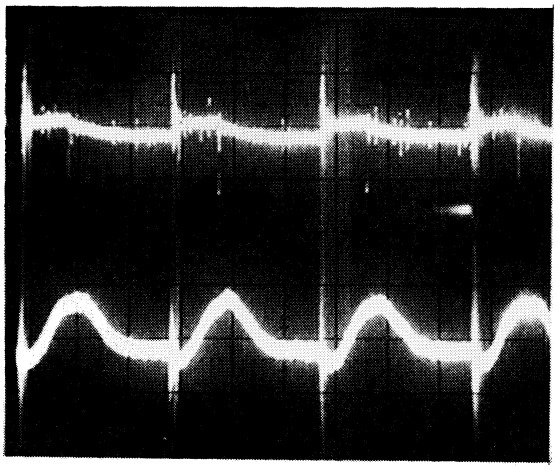

Figure 3. Power line conducted interference. Upper trace: interference on power line (1V/Div). Lower trace: interference at speaker terminals (0.05V/Div). Time base: 5ms/Div.

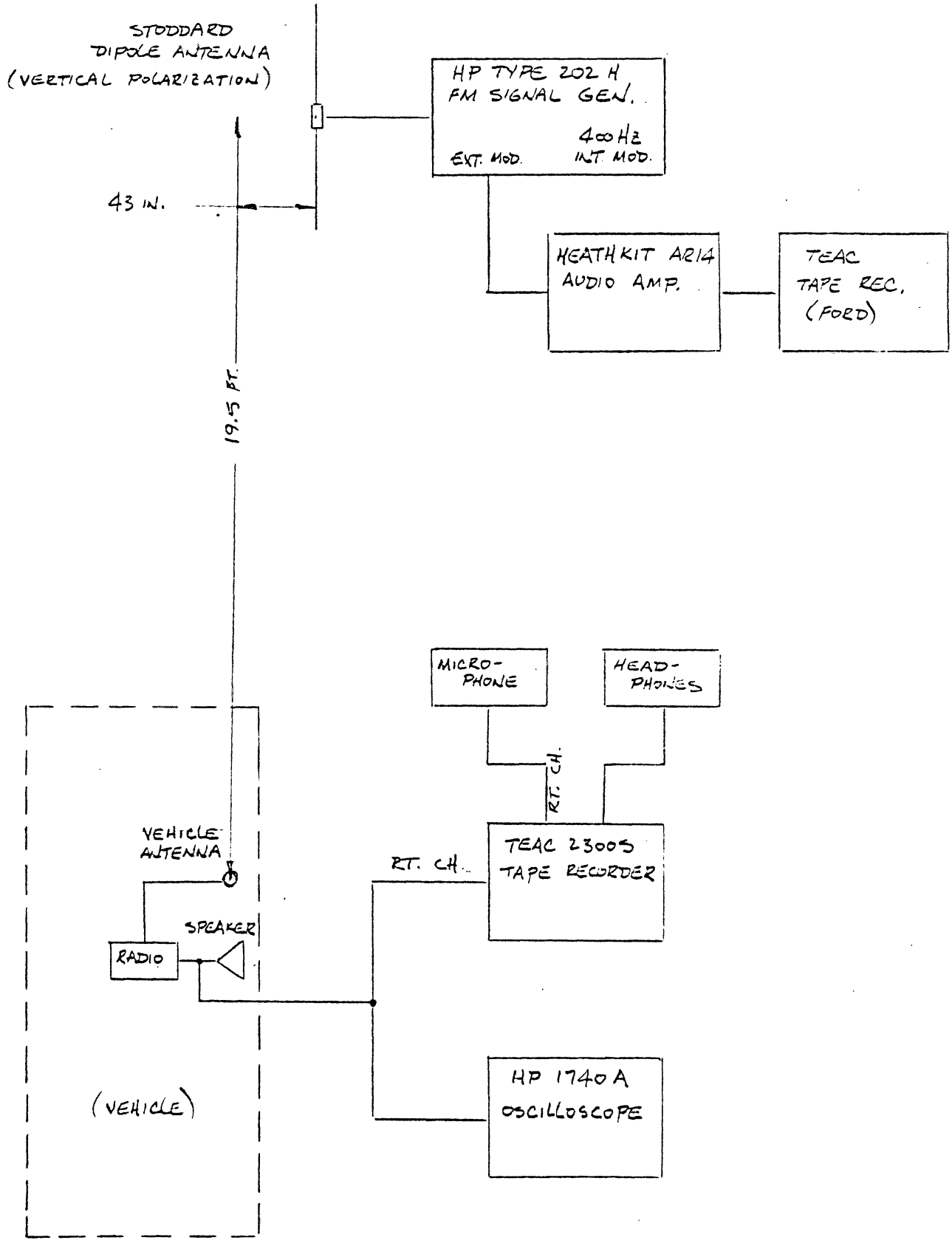

Figure 4. Test set-up for measuring radiated interference

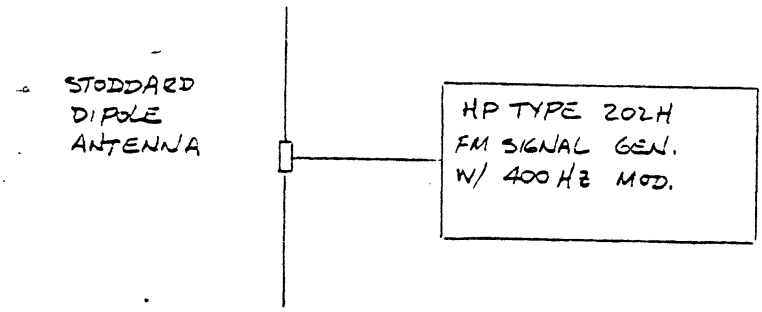

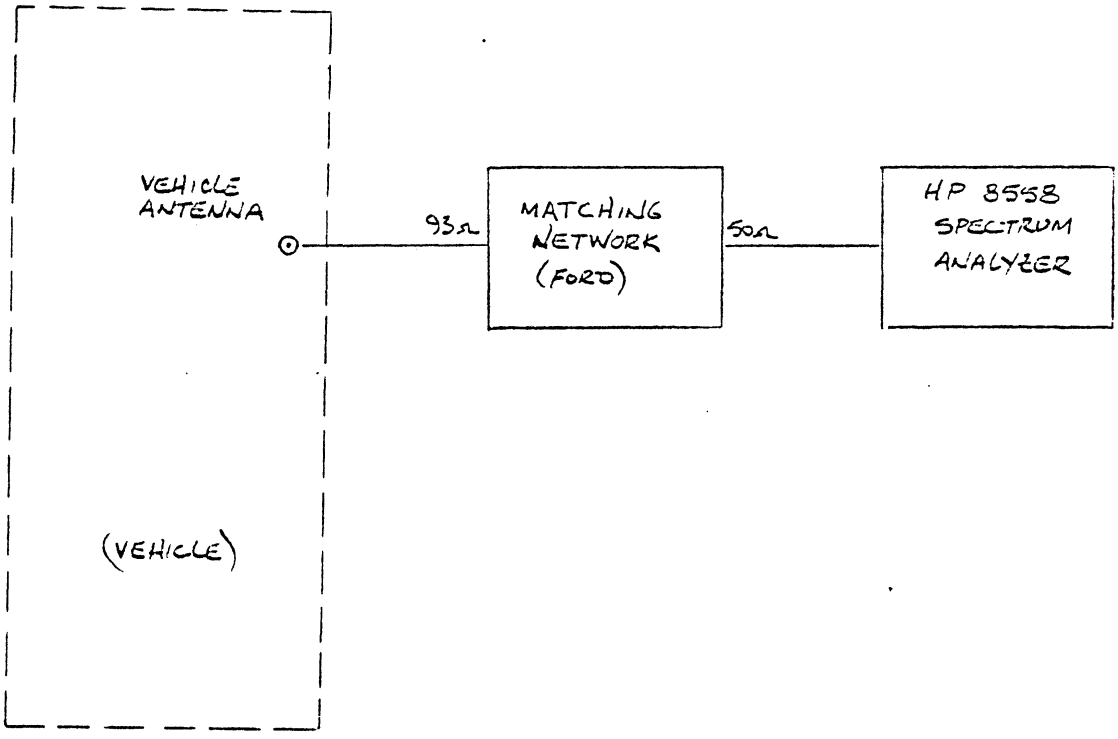

Figure 5. Test set-up for measuring RF carrier level

(An RF voltmeter or other similar instrument cannot be used to measure the carrier level due to the presence of FM broadcast signals). Assuming the antenna to have an impedance of 100 Ω, the generator was adjusted to provide a level of -90 dBm into 50 Ω as measured by the spectrum analyzer. This corresponds to 28 μV at the antenna output terminals. Once this level was established, the vehicle antenna was reconnected to the radio. Because of the impulsive nature of the radiated fields generated by the vehicle and the presence of FM broadcast signals, analysis of the actual interference signals at the antenna terminals was not feasable and measurements were therefore limited to the noise signals produced at the speaker terminals. The results show that the ignition system and instrument voltage regulator (IVR) are the primary sources of radiated interference, with the former being by far the more dominant. The IVR interference shown in Figure 6 was measured with the vehicle ignition switch on but the engine not operating. It is seen that the noise is impulsive in nature with peak values of approximately 150 mV. Under normal vehicle conditions, IVR interference is aperiodic and infrequent. It is,however, quite sensitive to mechanical disturbances within the vehicle, and for purposes of illistration the repetition rate of the noise shown in Figure 6 was enhanced by tapping on the vehicle dashboard. Figure 6 may therefore be considered as representing a "worst case" condition for IVR interference. The interference caused by the ignition system when the engine is operating is illustrated in Figure 7. The ignition noise also has an impulsive character, but it is much greater in amplitude (peak values of approximately 700 mV) than the IVR noise and it is repetitive with a period of approximately 15 ms. It is not, however, periodic in a strict sense since there are variations in both the amplitudes of the noise impulses and the time intervals between them. Although the ignition noise shown in Figure 7 predominantly consists of negative-going voltage impulses, it is noted that during some measurements the noise impulses were predominantly positive-going or were a mixture of positive and negative impulses. This anomaly will be further discussed in section 2.3.

Despite the fact that the two test vehicles were identical from a manufacturing viewpoint, the level of audio noise was found to be much greater in vehicle 526 T 129. The ignition noise in this vehicle exhibited peak values of 700 mV compared to only 200 mV in vehicle 526 T 130. To determine whether this difference was attributable to differences between the vehicle radios, another radio was placed in vehicle 526 T 129. This test radio was positioned

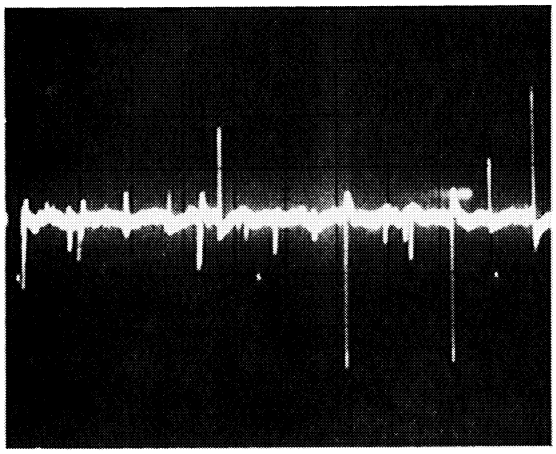

Figure 6. Radiated interference from IVR
Vertical: 0.05V/Div Horizontal: 10ms/Div

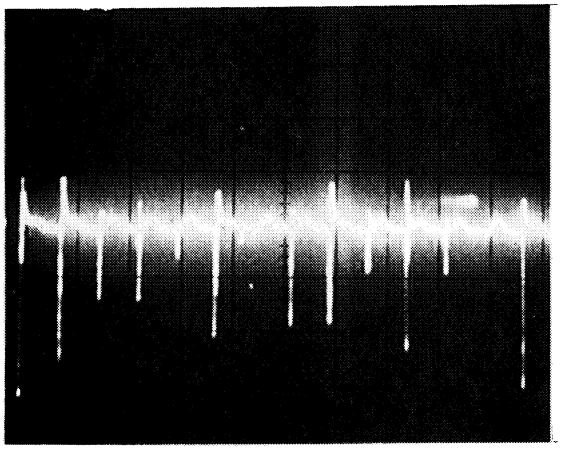

Figure 7. Radiated interference from ignition system
Vertical: 0.2V/Div Horizontal: 20ms/Div

near the original vehicle radio but was not actually installed in the dashboard as a replacement. Performance of the two radios was judged to be the same, i.e. approximately the same levels of IVR and ignition noise were measured in each radio. The difference in the levels of radio interference must therefore be attributed to some inherent difference between the two vehicles. Since there is presently some question as to whether or not present methods of measuring ignition radiation (see section 4.1) can be correlated with radio interference, it would be of interest to compare the test vehicles on the basis of ignition radiation measurements made in accordance with SAE J551c[1]. Such measurements were scheduled during the investigation but were not carried out due to the limited availability of the test vehicles.

2.3 Ignition Radiation

On the basis of the preceding results, radiation generated by the ignition system and coupled to the vehicle antenna is the primary source of RFI and was therefore investigated in further detail. The probable cause of the time variations between noise impulses is a variation in the engine speed. This hypothesis was proven correct by placing current probes on the spark plug cables to show that the noise impulses are synchronous with ignition events in the engine and that the time interval between these events has the same variation as the time between noise impulses. An analogous explanation for the noise amplitude variations could not be obtained. If it is assumed that each cylinder has a distinct radiation characteristic, then it may be expected that the ignition noise would display a pattern which repeats itself with every complete cycle (two revolutions) of the engine. However, no such pattern was observed. In fact, the data obtained for a single cylinder of the engine showed that not every ignition event produced a noise impulse in the output of the radio, and those noise impulses which did occur had a random amplitude distribution. This suggests a non-linear response within the radio itself, since it is doubtful that such large variations in the noise amplitude could be entirely accounted for by the cycle to cycle variations of the combustion process or the ignition system. The dependence of ignition noise on the carrier frequency was also examined. For a fixed carrier level, the ignition noise was greater at 90 MHz than at 105.5 MHz, indicating either that the radio is more susceptable to RFI at the low frequency end of the FM band or the spectral intensity of the vehicle interference is greater in that region.

The two test vehicles provide valuable samples of the actual ignition noise, but they afford no means by which to control the level of radio interference. With the radio set to standard test conditions, each vehicle has a single characteristic interference level. In order to obtain more controlled test conditions and to gain some insight into the nature of the interference generated by the ignition system, the ignition radition was simulated using an impulse generator as shown in Figure 8. The output of the impulse generator consists of rectangular voltage pulses of positive or negative polarity having variable amplitude and a time duration of 0.6 ns. The period was adjusted to 15 ms to simulate an engine speed of 1000 RPM. The spectral content of these pulses, obtained from their Fourier series representation (see Appendix A), is flat throughout the FM broadcast band. This simulation technique produced radio interference which was essentially the same in terms of both voltage waveform and audio perception as that measured previously due to operation of the test vehicles. By tuning the radio and FM generator to selected frequencies and measuring the interference, it was found that the noise level in the radio output was independent of the test frequency. This result, combined with the results of previous measurements, imply that the spectral distribution of ignition radiation in the two test vehicles was greater in the low frequency region of the FM band. Reversing the polarity of the output of the impulse generator had no effect on the radio interference. However, it was observed that both the amplitude and polarity of the noise impulses produced at the radio output are dependent upon how accurately the center tuned frequency of the radio is matched to the carrier frequency. Denoting these frequencies by f_c and f_o respectively, the radio interference is minimum when $f_c = f_o$ and increases in amplitude and frequency as the radio is detuned. The audio noise consists of positive-going impulses when f_c is less than f_o and of negative-going impulses when f_c is greater than f_o. Because of the complications introduced by FM broadcast signals and other ambient electromagnetic radiation when using radiated test signals, the test set-up was modified to that shown in Figure 9. All of the above results were reproduced without change. The interference produced by pulses having an amplitude of 30 V (measured at the output terminals of the impulse generator) is shown in Figure 10 for the cases $f_c < f_o$, $f_c = f_o$ and $f_c > f_o$. Although the interference is produced by voltage pulses of constant amplitude, the resultant noise impulses still exhibit a large amplitude variation.

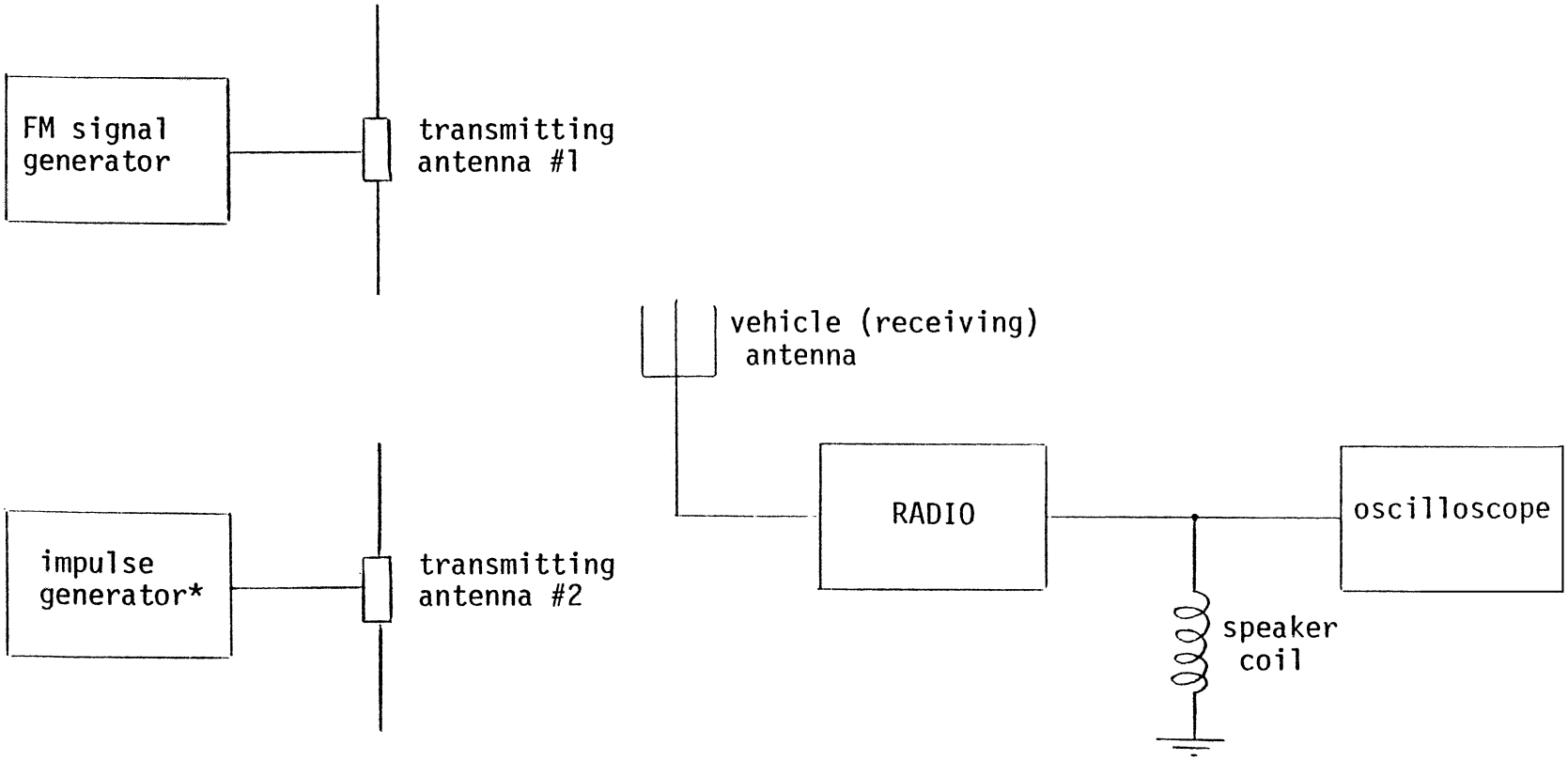

*Spencer-Kennedy Laboratories, model 503A

Figure 8. Simulation of interference produced by ignition radiation using radiated test signals

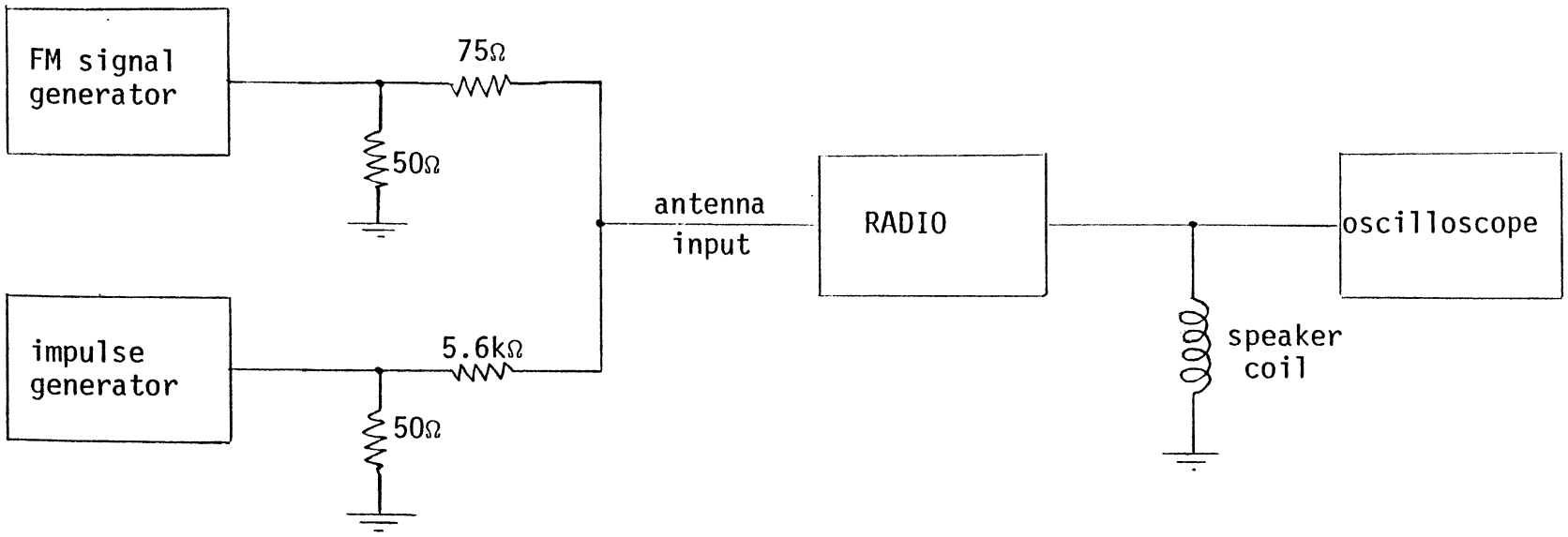

Figure 9. Simulation of interference produced by ignition radiation using conducted signals

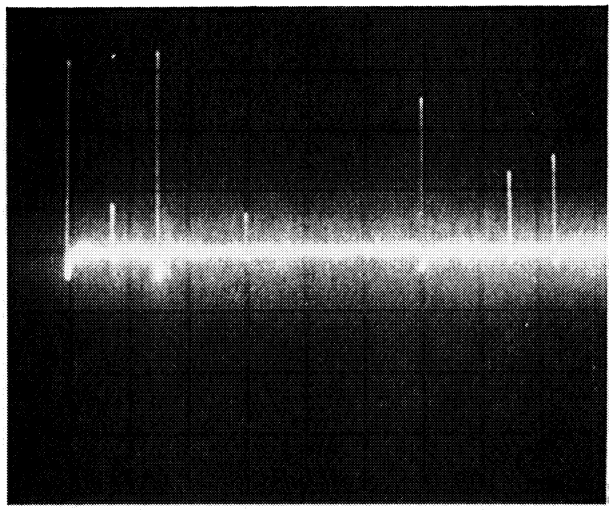

(a) f_c = 100.752 MHz f_o = 100.852 MHz

Figure 10. Dependence of noise signal on accuracy with which the radio is tuned to the RF carrier.
Vertical: 0.5V/Div Horizontal: 20ms/Div
(Ignition interference was simulated using the test set-up shown in Figure 9)

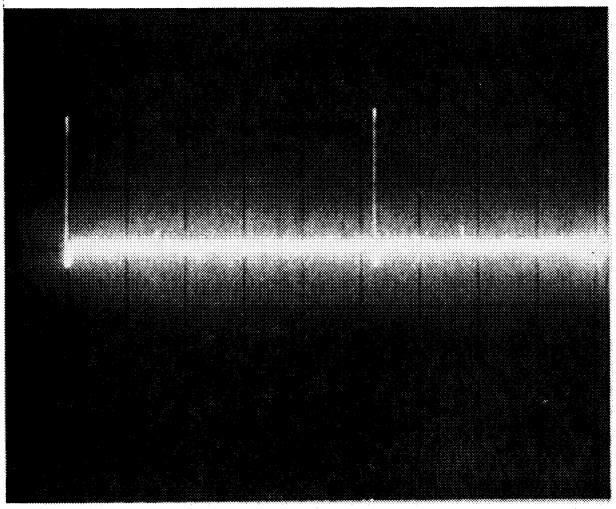

(b) $f_c = f_o = 100.75$ MHz

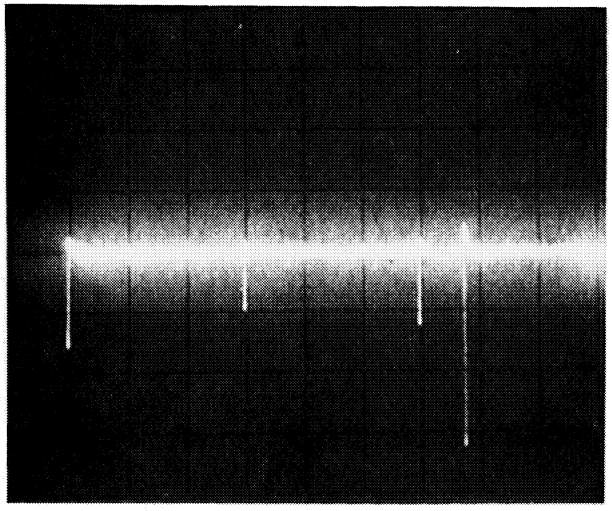

(c) $f_c = 100.752$ MHz $\quad f_o = 100.652$ MHz

3. MEASUREMENT OF AUDIO NOISE

This part of the investigation was directed toward the development of methods for obtaining objective measurements of audio degradation which can be correlated with the subjective evaluation of radio performance as perceived by the listener. Achievement of this objective first required a detailed analysis of the audio noise produced in the radio by operation of the vehicle. Based on this analysis, several measurement methods were examined and electronic circuitry was designed and built to implement that method considered to be most effective.

3.1 Audio Noise Analysis

During the investigation of RFI sources discussed in section 2, the radio interference produced by operation of the test vehicles was recorded on magnetic tape for later analysis (refer to Figure 4 for the test set-up). Prior to making any recordings of interference, the recording system itself was tested for susceptibility to vehicle interference to ensure that all tapes would be free of noise inherent to the test set-up and contain only those signals present at the speaker terminals and generated by the radio. The lead section of each tape was then used to record the 400 Hz modulating tone and the remaining portion of the tape used to record the audio noise with the RF carrier unmodulated. Playback of the recorded noise signal at the same volume level as the original signal could then be obtained simply by adjusting the gain of the playback amplifier to reproduce the 400 Hz tone at a peak-to-peak level of 1.5 V. This capability is particularly important when attempting to correlate electrical or acoustical noise measurements with subjective evaluations of the noise.

The electrical noise at the speaker terminals contains components attributable to power line conducted interference and radiated interference from the IVR and ignition system. Their time domain representations are given in Figures 3, 6 and 7 respectively and have already been discussed in some detail.

Frequency domain analysis of the noise was obtained from the tape recordings using the test set-up shown in Figure 11. Due to the limited gain of the tape recorder preamplifiers, a separate audio amplifier would have been necessary to reproduce the recordings at their original level and provide sufficient power to drive a speaker system. Since this might cause some distortion of the recorded signal, it was felt that a more accurate spectral analysis would be obtained by directly measuring the output of the tape recorder with the 400 Hz tone reproduced at a peak-to-peak level of 0.6 V. Consequently, the amplitudes measured were less than their "true" values by a multiplicative factor of 0.4 (or equivalently, an additive factor of -8 dBV). The results show that the spectral intensity of the noise is maximum near 1 KHz and decreases logarithmically with increasing frequency. At 8 KHz the spectral intensity has decreased by 30 dB or more from its value at 1 KHz. Measurements made with and without the 400 Hz modulating tone confirm that the noise spectrum is unaffected by carrier modulation.

The audio noise was modelled mathematically as the periodic function shown in Figure 12. It is noted that the dominant component of the audio noise was that radiated by the ignition system, and the model is based entirely on that component. The remaining components due to conducted and IVR interference have been neglected. Although the amplitudes given are based on a specific tape recording in which the noise consisted of negative-going voltage impulses, the waveform is representative of ignition noise in general. The model for noise consisting of positive-going voltage impulses is simply obtained by inverting the waveform. The frequency spectrum of the function shown in Figure 12 was obtained by Fourier analysis (see Appendix B) and compared to the measured spectrum of the tape recording. The computed spectrum of the simulated noise signal is plotted in Figure 13 and lies below the measured spectral distribution of the recorded audio noise. Assuming that the simulated signal is representative of the noise due to ignition radiation, there are several factors contributing to the differences between the two spectra. A period of 15 ms implies that the ignition noise spectrum is composed of discrete frequency components which are separated by intervals of 67 Hz. However, the measured noise spectrum was obtained using a spectrum analyzer bandwidth (3 dB) of 30 Hz. Since the impulse bandwidth of the spectrum analyzer is approximately equal to its 6 dB bandwidth, it is probable that two frequency components were actually measured for a given tuned frequency of the analyzer, thus accounting

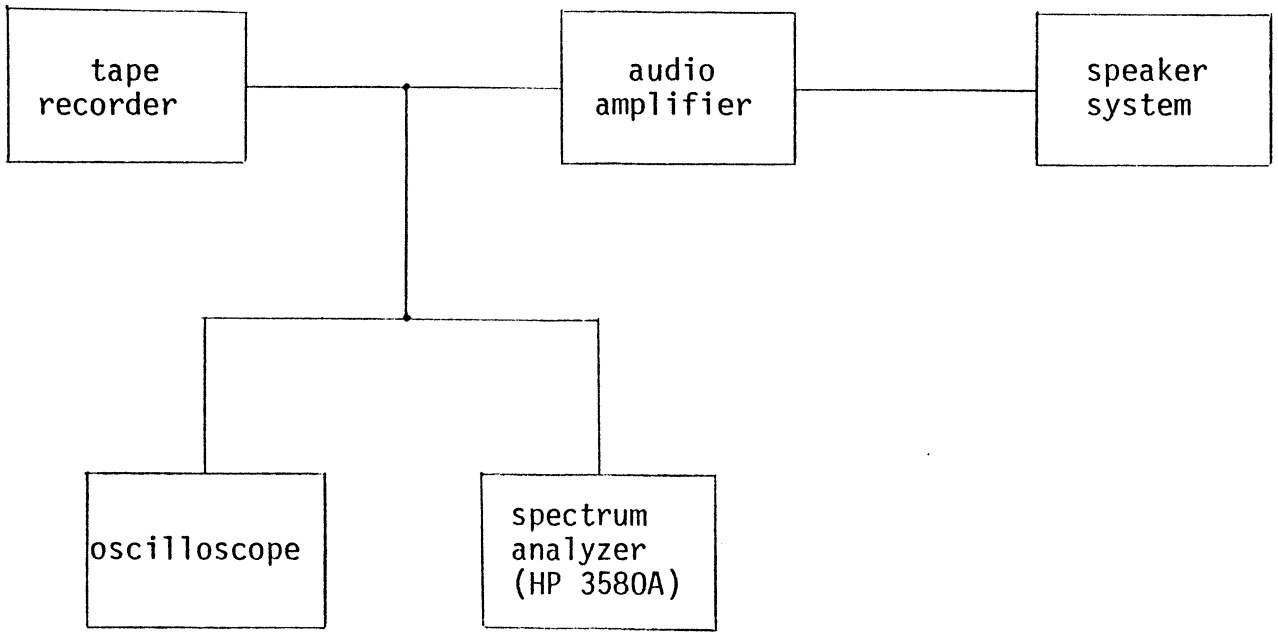

Figure 11. Test set-up for playback and analysis of tape recordings

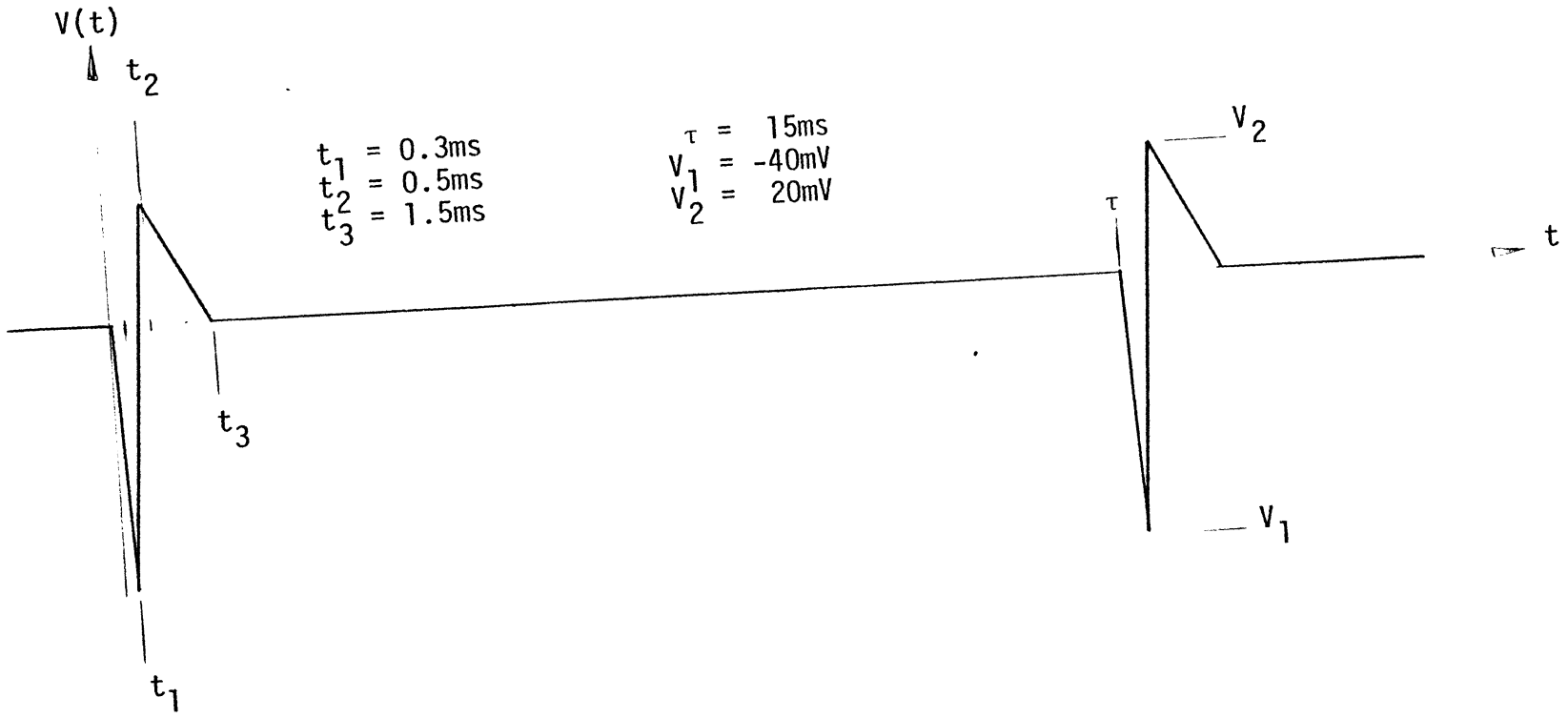

Figure 12. Mathematical model of audio noise produced by radiation from ignition system

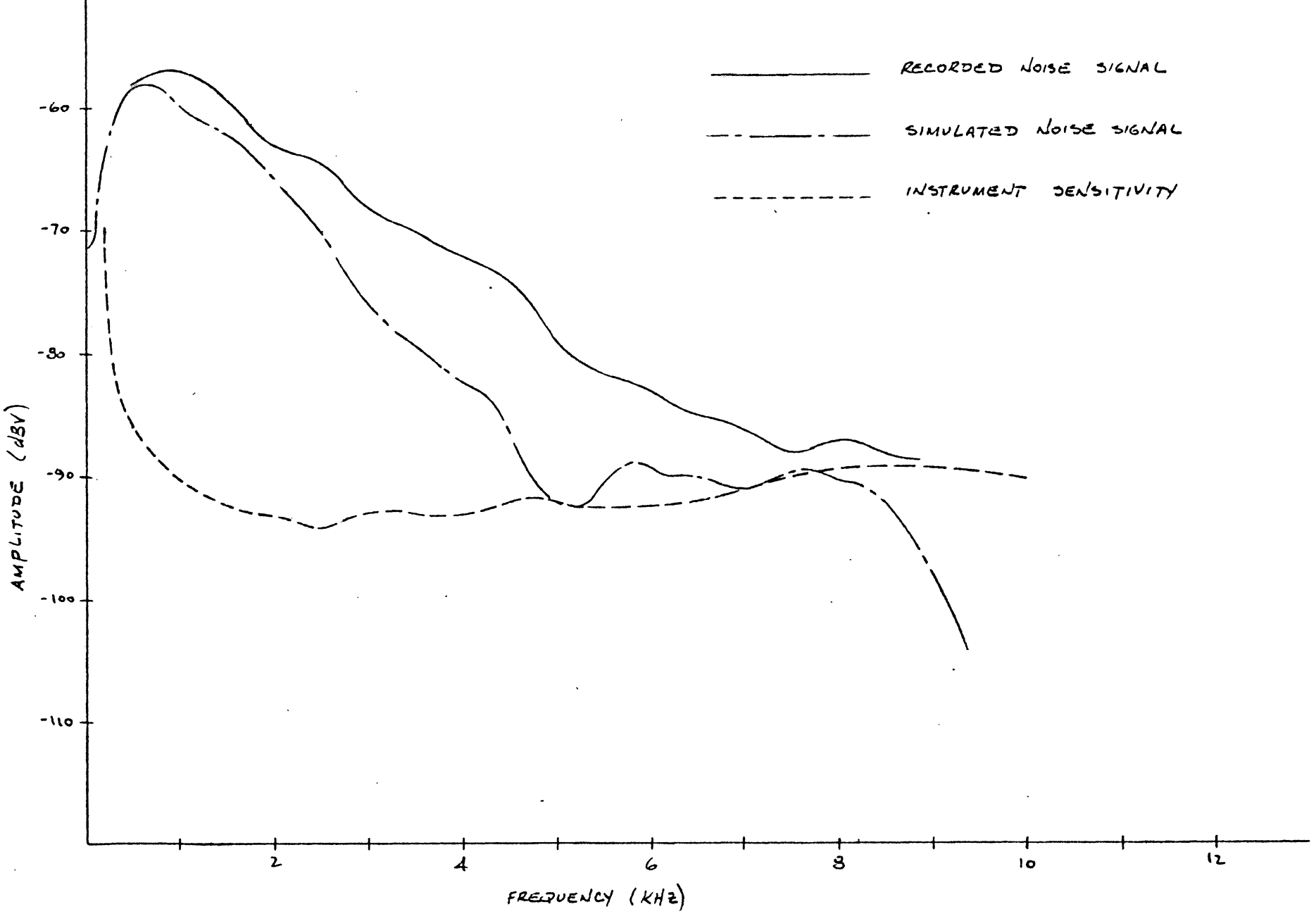

Figure 13. Spectral distribution of audio noise

for 6 dB of the difference between the spectra. However, this still leaves the measured spectrum significantly higher in the range 3 KHz to 6 KHz. This must be attributed to the presence of conducted and IVR noise components and the thermal noise of the radio as well,as the fact that, as noted earlier, the actual ignition noise is not a strictly periodic function.

Circuitry was designed and built to generate the noise signal shown in Figure 12 and adjustments provided so that the parameters t_1, t_2, t_3, τ, V_1 and V_2 could be varied. When this simulated signal was applied to an audio system and subjectively compared to the recorded audio noise, the main differences noted were the extreme periodicity of the simulated noise signal and the absence of background thermal noise superimposed over the interference. Despite these differences, the circuit provided an adequate simulation of the audio noise and was used extensively in the development of measurement techniques.

3.2 Measurement Techniques

The relative merits of electrical versus acoustical coupling were first evaluated. The tape recordings were played back through an audio amplifier into speakers of the type used in the test vehicles. A microphone was positioned in front of one speaker and both the speaker and microphone were placed inside an anechoic enclosure. The voltage waveforms at the speaker terminals and the microphone output were observed on an oscilloscope. The single advantage of acoustical coupling was found to be that it takes into account the dynamic response of the speaker. However, this advantage is minimal because most of the electrical signals at the speaker terminals are within the range of the speaker response and therefore were also present in the microphone output. Disadvantages of acoustical coupling are its sensitivity to the distance and direction of separation of the microphone from the speaker and the requirement of an anechoic enclosure. The need for an enclosure makes measurements within a vehicle impractical, but without the enclosure the measurements are influenced by the acoustical characteristics of the passenger compartment and are susceptible to the acoustical noise which is present when operating the vehicle. For these reasons, acoustical coupling was discarded in favor of direct electrical measurements at the speaker terminals.

Since it is desirable to obtain noise measurements which can be correlated with subjective evaluations of the radio, weighting networks were considered in order to obtain a measuring instrument which duplicated the response of the human ear. There are three frequency response curves, designated A, B and C, [2] which are commonly used in audio noise measurements. The A weighted response is most representative of the response of the human ear, and of the various weighting schemes which have been tried in the past, it has provided the most successful results.[3] However, the spectral analysis of the preceding section shows that the audio noise lies predominantly within the range 500 Hz to 8 KHz. Since the A weighted response is relatively flat throughout this range, the weighting network should have little effect on noise measurements. This was verified experimentally using flat response and A weighted networks. No observable difference was found between the two cases, and it was therefore concluded that the incorporation of special weighting networks into the measuring instrument was not necessary.

The next task was to determine which parameters of the noise signal should be measured. The parameters chosen must provide a good correlation with the subjective scale of one through ten presently used by Ford Motor Company, and must also be measurable in a straightforward manner with good noise sensitivity and resolution. Commercially available distortion analyzers and sound level meters typically measure either the power level or RMS voltage of the noise. However, these parameters are more suitable for application to random (white) noise or continuous wave (cw) interference and do not provide an adequate measure of the impulsive noise in the radio output. For example, a General Radio model 1551C sound level meter was used to measure the levels of both recorded and simulated noise signals. The measurements of the recorded audio noise were approximately 20 dB higher than the corresponding measurements of a simulated noise signal which was set subjectively to the same level; and doubling the perceived level of the noise, which according to King[4] should increase the measurement by 10 dB, produced only a slight increase in the meter reading. These conflicting results are attributable to the fact that the sound level meter employed an RMS detector. The noise perceived by the listener is dominated by the impulsive ignition noise. Although the ignition noise has an amplitude which is large relative to the background thermal noise, its small duty cycle results in an RMS value which is not large compared to that of the background noise.

After comparing subjective evaluations of the tape recordings with oscilloscope measurements taken at the speaker terminals, it was concluded that the best indication of the audio noise level was the average peak-to-peak amplitude of the noise impulses over a specified time interval. Of course, the replacement of a discriminating audiophile by a simple electronic circuit is a rather formidable task, and some degree of compromise must be tolerated. The objectivity gained by measuring the single parameter indicated is obtained at the expense of the ability to discriminate between noise signals which have the same average level but do not produce the same effects in terms of annoyance when judged subjectively. For example, the averaging process, which is made necessary by the large amplitude variation in the noise impulses, means that ten noise impulses of unity amplitude occurring during the specified time interval would be assigned the same noise level as a single impulse having an amplitude of ten. It is unlikely that a listener would perceive these two situations as identical. Nevertheless, this parameter can be measured without difficulty and is expected to provide adequate correlation with subjective evaluations. More complex methods of signal processing might possibly lead to improved results, but would be inconsistent with the present goal of providing a relatively simple compact test instrument for evaluation.

3.3 Instrument Design

Electronic circuitry was designed and built for measuring the average peak-to-peak amplitude of impulsive noise signals at the radio speaker terminals. A block diagram and circuit schematic are shown in Figures 14 and 15 respectively and typical voltage waveforms are plotted in Figure 16. The circuit board layout given in Figure 17 will be of assistance if it is necessary to adjust any of the circuit parameters. Noise measurements are made by simply connecting the circuit imput to the radio speaker terminals (proper polarity must be observed) and connecting the output to a DC voltmeter. The instrument requires a dual ± 15 VDC power supply, and care should be taken that power to the circuit is switched on before applying an input signal. Since the speakers have a nominal quiescent current of 50 ma, the input switch S_1 should be in the AC position. The DC position is used only when calibrating the instrument using a laboratory signal source, e.g. a pulse generator. A brief description of the circuit operation is given in the following paragraph.

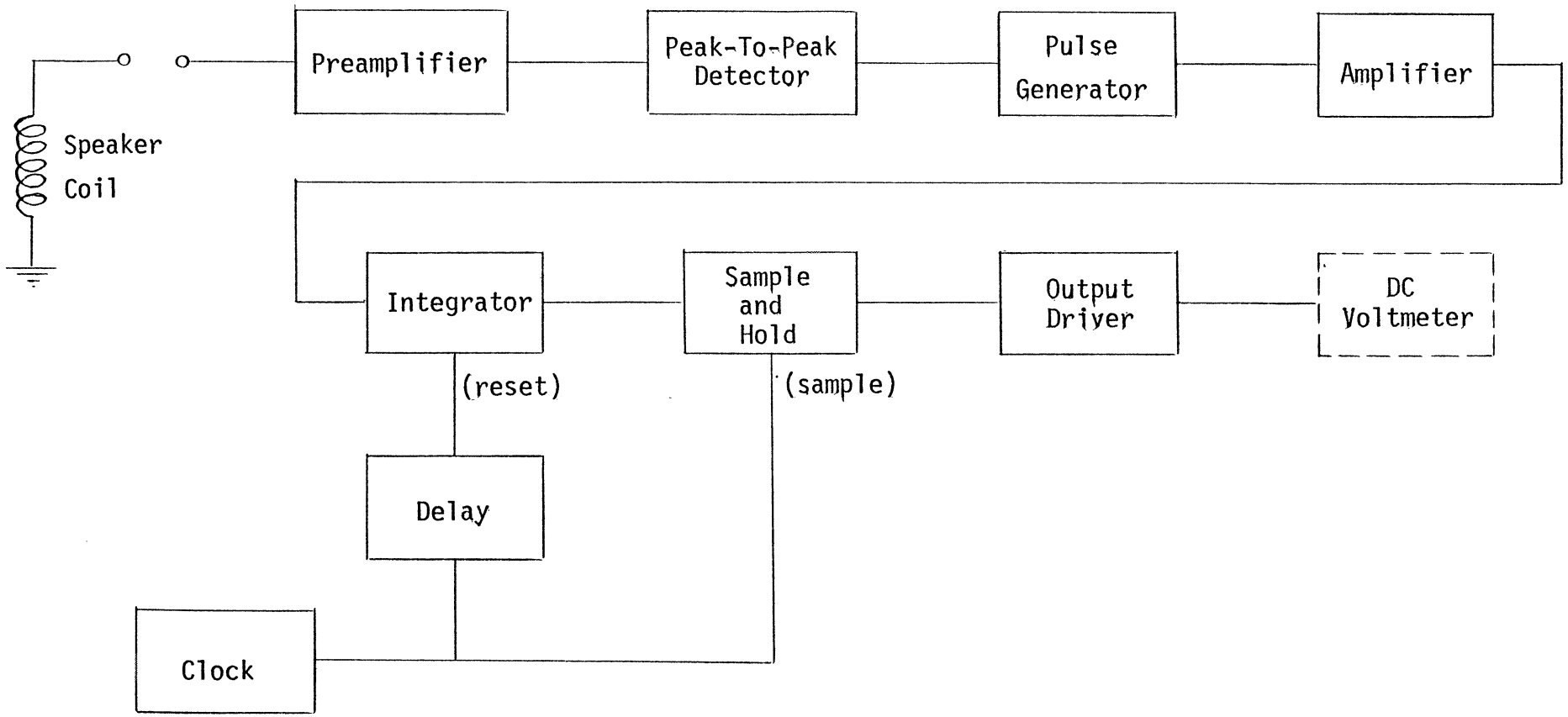

Figure 14: Block diagram of circuitry for measuring audio noise.

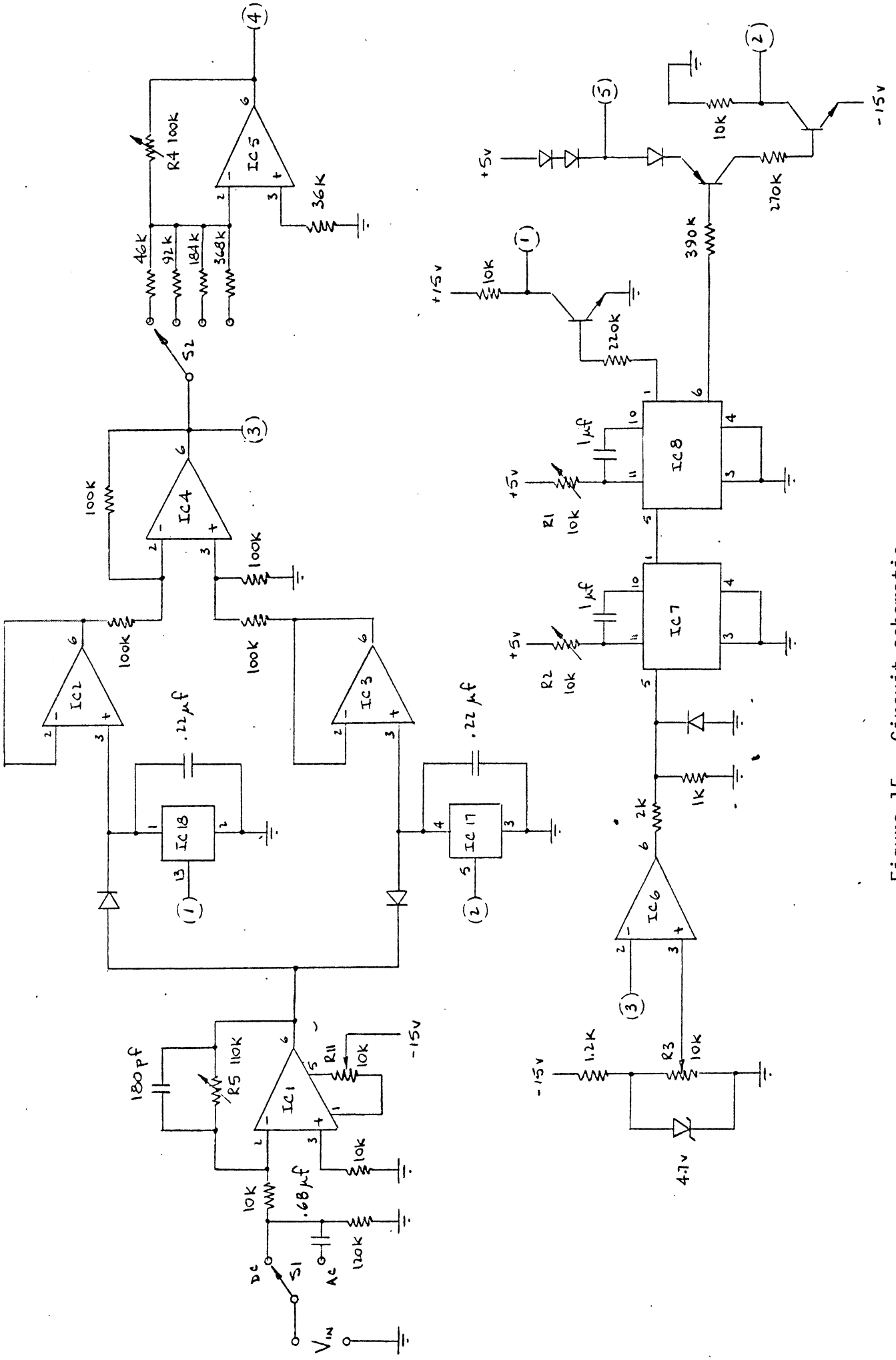

Figure 15. Circuit schematic

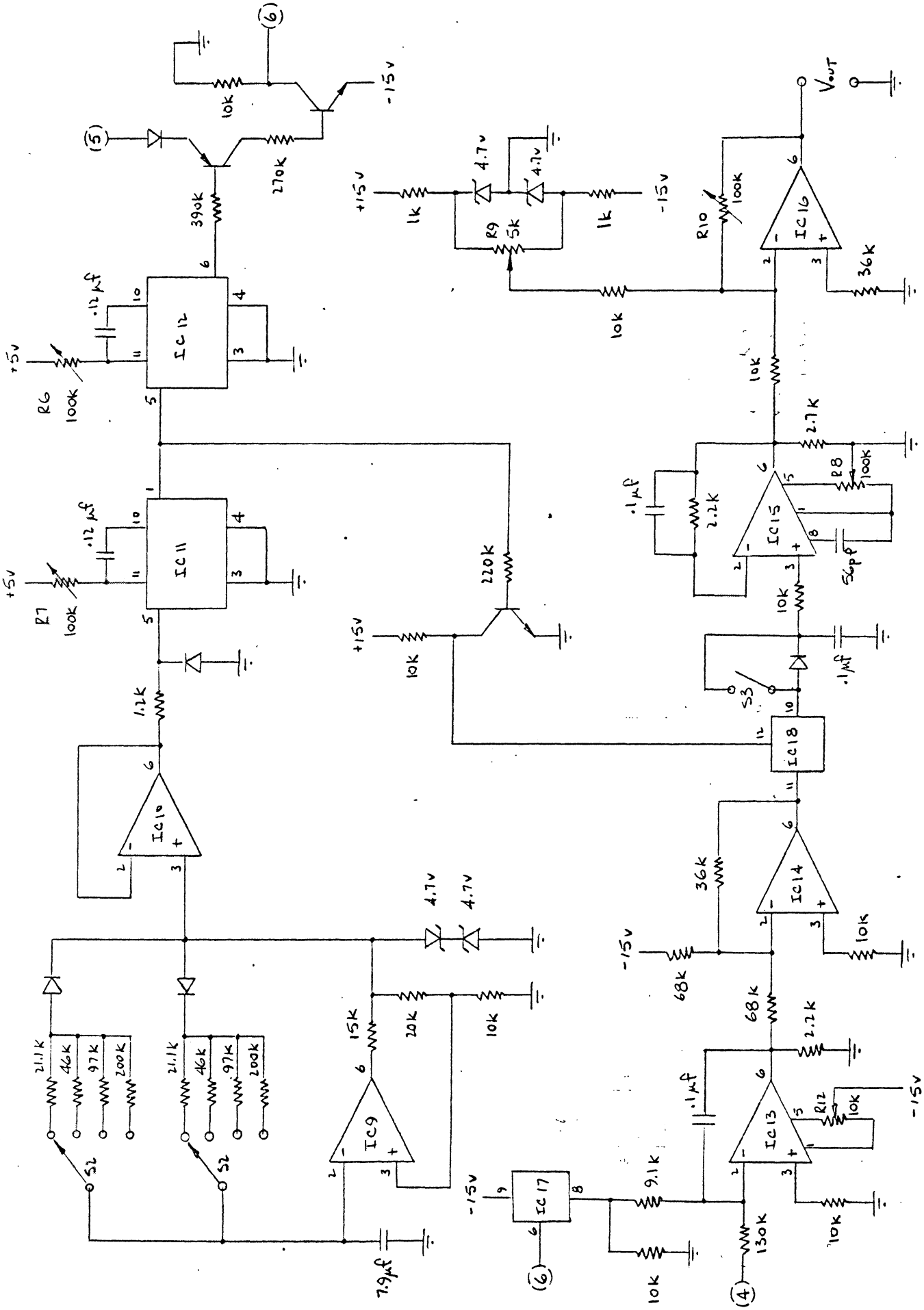

Figure 15. Circuit schematic (continued)

+5V DC POWER SUPPLY:

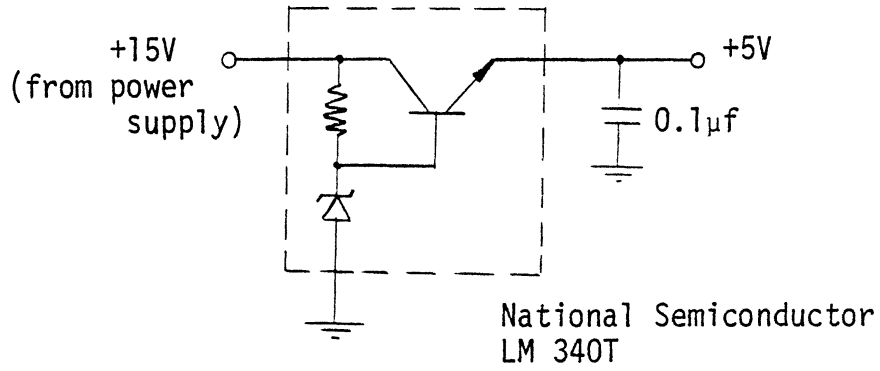

NOTES: (1) IC7, IC8, IC11, IC12 are monostable multivibrator circuits (Texas Instrument Sn 74121 or equivalent)

(2) IC15 is a COSMOS operational amplifier (RCA CA 3130). All other operational amplifiers are general purpose types (National Semiconductor μA741 or equivalent)

(3) IC17 and IC18 are quad bilateral switches (RCA CA4016 or equivalent). IC17 is operated with V_{DD} = 0, V_{SS} = -15V and IC18 is operated at V_{DD} = +15V, V_{SS} = 0

(4) the circuit requires a dual ± 15V DC power supply

(5) the power supply should be switched on before applying an input signal

Figure 15. Circuit schematic (continued)

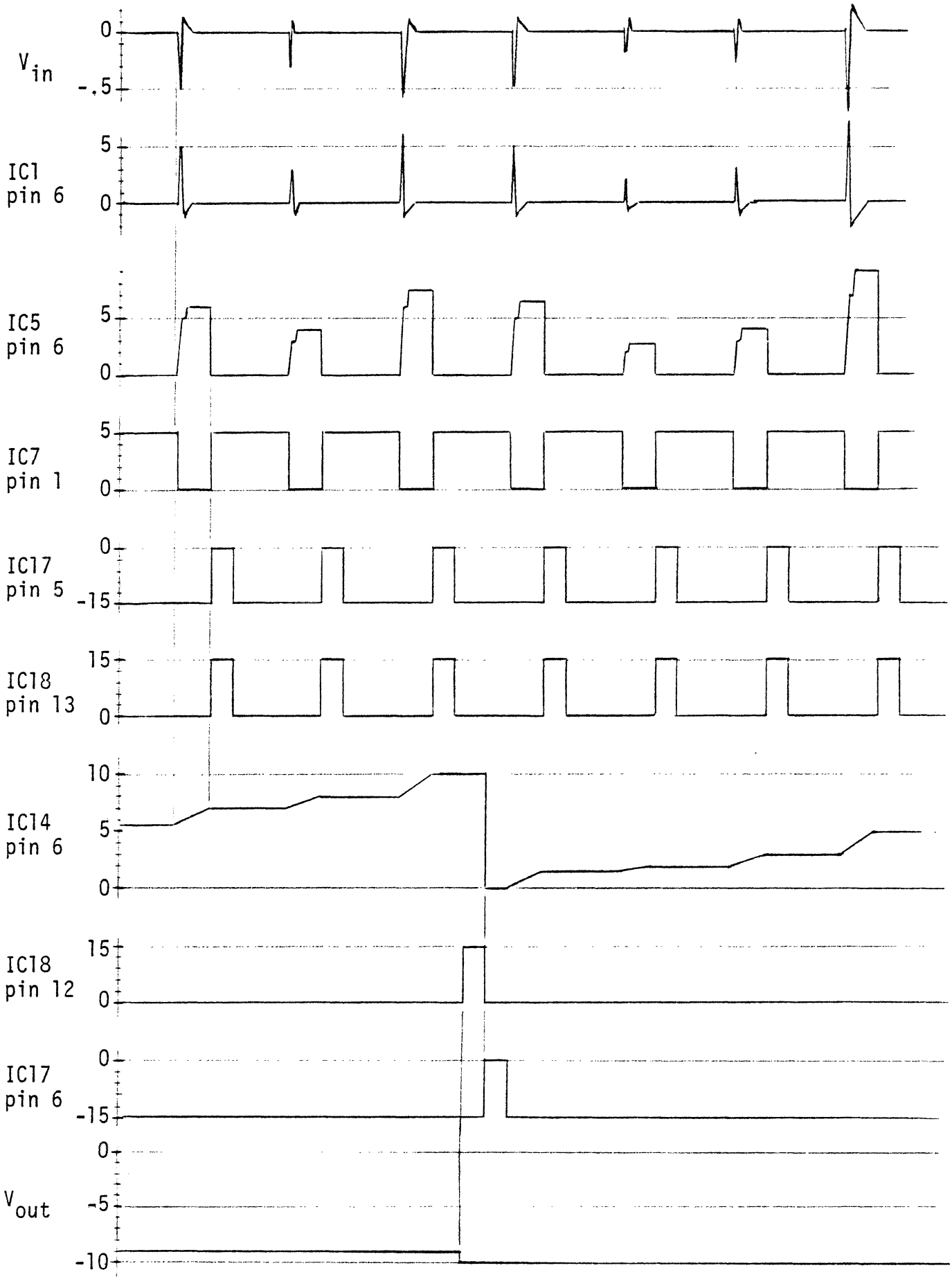

Figure 16. Typical voltage waveforms

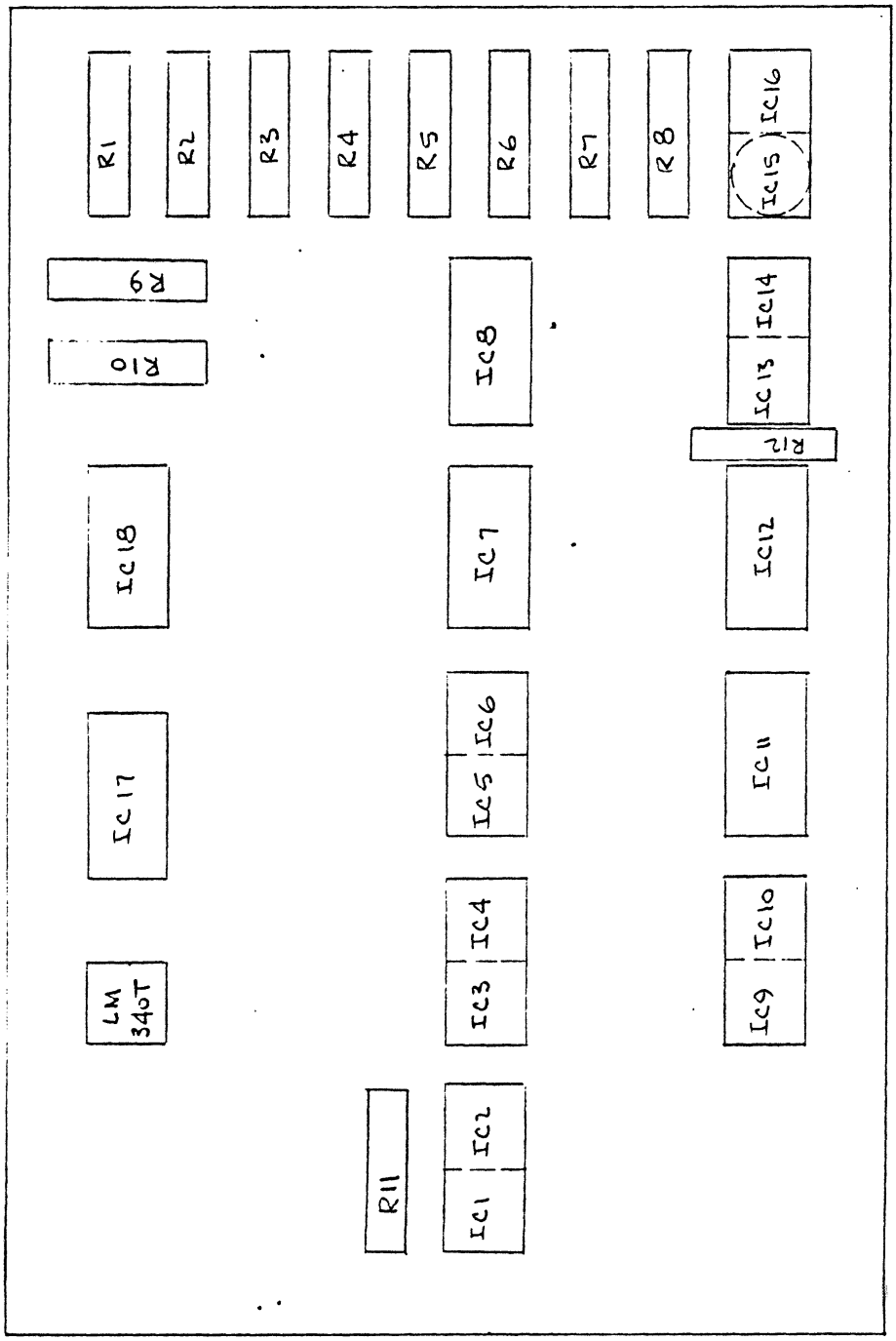

Figure 17. Circuit board layout

The input signal is applied to a preamplifier (IC_1) and then a peak-to-peak detector (IC_2, IC_3, IC_4). The output of the peak-to-peak detector is given by $V = - g_1 V_p$ where V_p is the peak-to-peak value of the noise impulse applied to the circuit input and g_1 is the gain of the preamplifier. The value of g_1 can be varied by adjusting R_5 and controls the sensitivity and dynamic range of the circuit. The value of V is held for a time t_2 (adjustable by R_2) and the detector output is then reset to zero until the next noise pulse occurs. Hence, the output of the detector is a series of rectangular pulses of width t_2 and having amplitudes proportional to the peak-to-peak level of the noise. The pulses are amplified by IC_5 (gain g_2 adjustable by R_4) and then integrated (IC_{13}, IC_{14}) for a time τ. The integration (sample) time τ is selectable as .25, .5, 1.0 or 2.0 seconds using S_2. Increasing either g_2 or t_2 will increase the output of the integrator. At the end of each integration the output of the integrator is sampled and held by IC_{15} and the integrator is reset for the next integration. The sampled voltage is applied to a driver (IC_{16}) which produces a negative DC output voltage whose amplitude is proportional to the average peak-to-peak value of the noise over the sample time τ. For convenience in displaying this output on a meter, the offset and gain of the driver can be adjusted using R_9 and R_{10} respectively. Due to the large amplitude variations and randomness in the ignition noise, the circuit output also varies, particularly for small values of τ. These variations can be damped, and the output weighted toward the higher level noise impulses by closing switch S_3 (slow response position).

The instrument was delivered to Ford Motor Company for evaluation on 3 June 1977. The circuit parameters were adjusted for $g_1 = 10$ and $t_2 = 4$ ms. All other amplifier gains were set to unity and monostable circuits adjusted for pulse durations of 2 ms. For an input signal having a 15 ms period, the circuit output under these conditions is given by $V_{out} = - 20 \overline{V}_p$ where $\overline{V}_p$ is the average peak-to-peak voltage of the noise impulses occurring during the time interval τ. It is remarked that the instrument was designed for use with the radio set to standard test conditions as specified in section 2.1 and with the engine operating at 1000 RPM (2000 RPM for four cylinder engines). Since the sample time τ is independent of engine speed, the circuit output increases proportionally with increasing engine speed. This variation can be eliminated if desired by replacing the present clock circuit with a divide by N counter with a trigger circuit synchronized to spark ignition. The sample time τ would then be an integral number of engine cycles regardless of engine speed.

4. PREDICTION AND MEASUREMENT OF RFI

Since ignition radiation is the dominant RFI source, present day techniques for measuring ignition radiation are reviewed and the applicability of their results to prediction of radio interference is evaluated. An alternative RFI measurement system is described which uses the audio noise instrumentation discussed in section 3.3 and is intended specifically for the case where the radio is installed within the radiating vehicle.

4.1 Prediction based on ignition radiation measurements

Vehicle ignition systems produce impulsive radiation having a radio frequency spectrum which may extend as high as 7 GHz. Measurements obtained from a large sampling of the vehicle population indicate a broad maximum in ignition noise impulse field strength in a region centered about 300 MHz which is generally thought to occur because the vehicle radiates more efficiently at these frequencies. Most of the results obtained to date have relied upon the measurement techniques specified in SAE J551c and have been concerned primarily with interference of the land mobile communication services. This means that evaluations are based on inteligibility of voice communication rather than fidelity. Even when using this less critical parameter, test results have indicated that a significant number of motor vehicles do produce interference effects.[5] However, no satisfactory method has been found by which to correlate the level of radio degradation with the peak and quasi-peak measurements of ignition radiation. In an effort to improve this situation, special equipment has recently been designed at Stanford Research Institute[6] to measure the strength and average rate of occurrence of impulsive radiation. Although this measurement technique, known as the noise amplitude distribution (NAD) method, is claimed to provide an improvement over peak or quasi-peak measurements, it has not yet been demonstrated that the results can be accurately correlated with receiver susceptibility tests to predict degradation.

It is also noted that simply maintaining the vehicle radiation within the limits specified by SAE J551c does not necessarily eliminate all RFI problems. For example, consider the simulated ignition noise discussed in section 2.3. Significant interference was observed at a frequency of 100 MHz with the pulse amplitude (measured at the antenna input terminals of the radio) set at approxiamtely 0.3 V. To compute the spectral intensity of the applied signal we first note that for $n = 15 \times 10^5$ (corresponding to $f_n = 100$ MHz)

$$A_n = \frac{2V}{n\pi} \sin \frac{n\pi T}{\tau} = 2.4 \times 10^{-8} \text{ V}$$

Since the spectral distribution is uniform in this region and there are 15 frequency components per kilohertz bandwidth, the spectral intensity is

$$S = \frac{15}{\sqrt{2}} A_n = 0.25 \ \mu\text{V/KHz}$$

The field strength limit at 100 MHz specified by SAE J551c is 14 dBμV/m/KHz. If we assume the receiving antenna to be a quarter wavelength monopole above a perfect ground plane, then the antenna gain and effective area are given by[7]

$$G = 3.28 \qquad A = \frac{\lambda^2 G}{4\pi}$$

where λ is the wavelength of the incident radiation. For free-space fields, $\lambda = 3$ m for $f = 100$ MHz and the received power available at the antenna terminals is

$$P = \frac{E^2 A}{120\pi}$$ where E is the RMS value of the incident electric field.

Assuming an antenna impedance of $R = 100\ \Omega$ and a matched load, the spectral intensity at the antenna terminals is

$$S_A = \frac{E\lambda}{4\pi} \left(\frac{GR}{30}\right)^{1/2} = 3.95 \ \mu\text{V/KHz}.$$

Even when the inaccuracies of some of the assumptions are taken into account, it is evident that with the radio set to standard test conditions, significant interference will be produced by ignition radiation which is well below the limits recommended in SAE J551c.

4.2 RFI Measurements for Vehicle-Installed Radios

We now address ourselves to the question of whether the methods cited above are applicable to the present investigation. First, it is noted that these methods are prediction techniques requiring separate measurements of the spectral intensity of the ignition radiation and the susceptibility characteristics of the radio system. Since a good correlation between these measurements has not been established, accurate predicitons of radio interference cannot be obtained. Second, the measurements are applicable only in the far field region, i.e. when the radio system is located ten meters or greater from the vehicle. These methods are therefore inappropriate for the present investigation where the radio is inside the radiating vehicle and its antenna is in the near field zone.

Although the standard measurement techniques could be extended to this case by placing a receiving antenna near the vehicle antenna, it is far simpler and more accurate to test the vehicle and radio as an integral system. This enables the actual interference levels to be determined from a single test and the results could be correlated with subjective evaluations of the radio interference by using the audio noise instrumentation described in section 3.3. The needs for elaborate receiving systems and additional tests to correlate field measurements with radio degradation are thus eliminated, and the fact that the radio antenna is in the near field zone is no longer a serious problem. Although the radio antenna should be mounted on the vehicle in its production configuration, the radio itself could be located remotely since it was found that all of the audible interference produced in vehicle-installed radios is attributable to radiative coupling to the vehicle antenna. The radiated RF carrier used in previous tests (see Figure 4) can be replaced by a carrier directly coupled from an FM signal generator. The proposed measurement system is shown in Figure 18. As in all previous measurements, the radio under test should be set to standard test conditions.

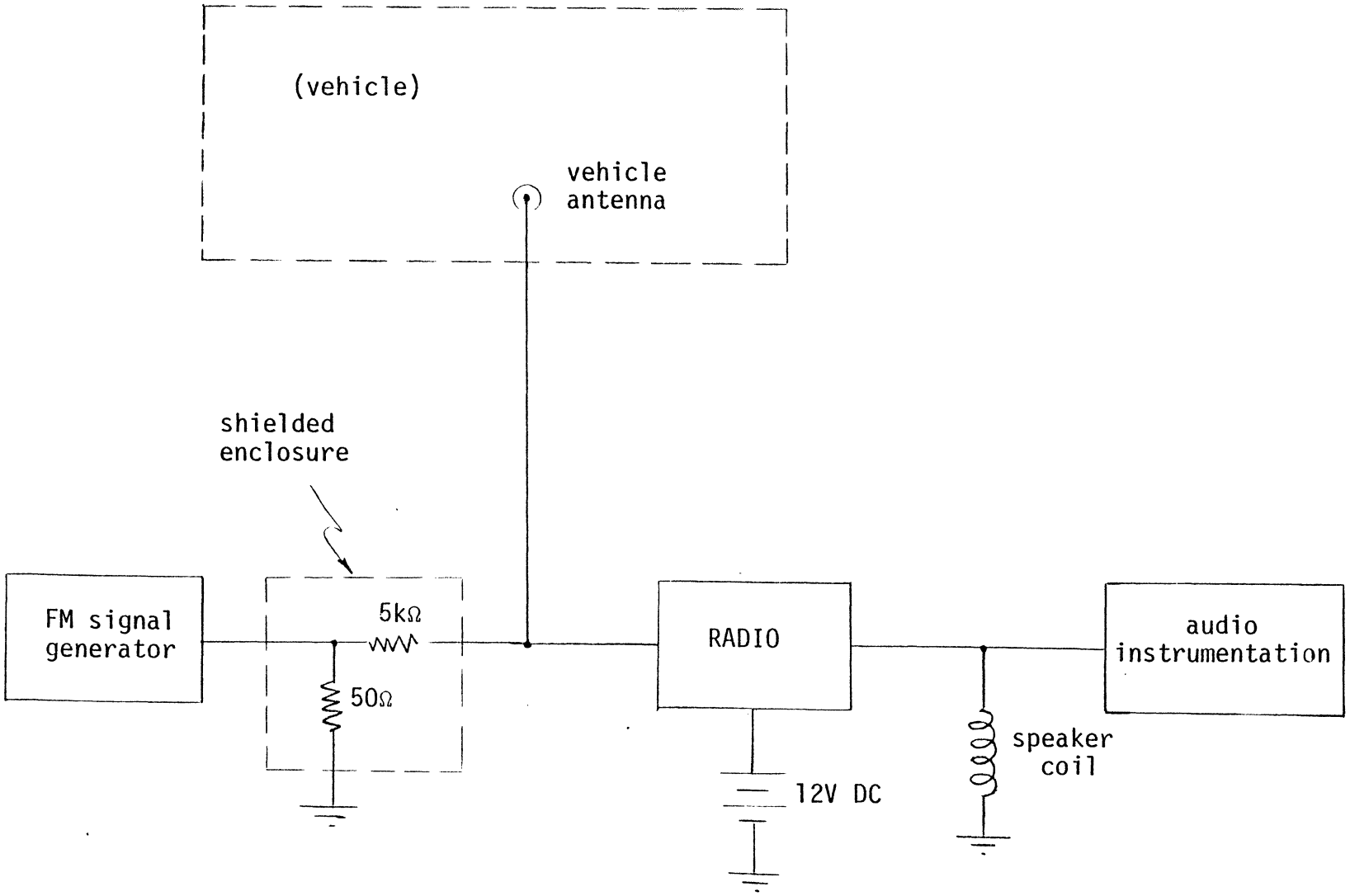

Figure 18. RFI measurement system for vehicle-installed radio systems. A setting of -37 dBm into 50Ω at the signal generator provide an RF carrier level of approximately 30 μV.

5. CONCLUSIONS AND RECOMMENDATIONS

The primary mechanism leading to audio distortion is radiative coupling of radio frequency interference (RFI) onto the vehicle antenna. A low level of power line conducted interference was present in the radio output but produced no audible noise. Neither radiative coupling to the speaker cables nor penetration of the radio chassis by electromagnetic fields produced any measurable interference.

The RFI coupled to the vehicle antenna was generated by the ignition system and the instrument voltage regulator (IVR) with the former being dominant. Both of these are impulsive noise sources with frequency spectra extending through the FM broadcast band. The exact manner in which the receiver detects these signals and produces audio noise is not known.

The impulsive audio noise at the radio speaker terminals reaches amplitudes as high as 700 mV and has a spectral distribution in the range of 500 Hz through 8 KHz with a maximum spectral intensity near 1 KHz. The level of audio noise is dependent upon the strength of the RFI source, the strength of the RF carrier and the accuracy with which the radio is tuned to the carrier. Based on analysis of the audio noise, it was concluded that the best correlation to subjective radio evaluations is obtained by measuring the average peak-to-peak amplitude of the noise impulses over a specified time interval.

Measurement of the acoustical noise rather than the electrical noise at the speaker terminals was found to be impractical and the use of SAE J551c or other far-zone measurements of vehicle radiation as a basis for predicting radio interference is inappropriate for vehicle-installed radios.

Since the present study has been limited to only two test vehicles, it is recommended that additional vehicles be tested. This may be done in part by Ford Motor Company during the course of evaluating the test instrument which has been supplied for measuring audio noise. The effects of antenna type and location on the level of radio interference should also be investigated and an explanation for the large difference in ignition noise between the two test vehicles used in the present investigation should be pursued. It is further

recommended that ignition radiation be studied in greater detail to determine the contributions made by the individual components of the ignition system and suppression techniques then developed for reducing radio interference.

ACKNOWLEDGEMENTS

The assistance of Messrs. I. Elrom and F. Rhine in the design and fabrication of required electronic circuitry and the performance of test measurements is gratefully acknowledged. The author is also indebted to Dr. D. L. Sengupta and Mr. J. E. Ferris for technical advice and discussions throughout the course of the investigation.

REFERENCES

[1] Society of Automotive Engineers Standard SAE J551c, "Measurement of Electromagnetic Radiation from a Motor Vehicle or other Internal Combustion Powered Device Excluding Aircraft (20 - 1000 MHz)".

[2] American National Standards Institute, ANSI 51.4 - 1971, "Specification for Sound Level Meters".

[3] Peterson, A.P.G. and E.E. Gross, Jr., Handbook of Noise Measurement, 7 ed., General Radio, Concord, Mass. (1967).

[4] King, A.J., The Measurement and Supression of Noise, Chapman and Hall, London (1965).

[5] Federal Communications Commission, "Motor Vehicle Ignition Radiation", OCE Report, Research and Standards Division, Office of the Chief Engineer, April 1976.

[6] Stanford Research Institute, "Measurement Parameters for Automobile Ignition Noise", Menlo Park, California, June 1975.

[7] Jasik, H., Antenna Engineering Handbook, McGraw-Hill, New York (1961).

APPENDIX A:

FOURIER SERIES REPRESENTATION OF SIMULATED IGNITION RADIATION

Consider the periodic function V(t) given by

$$V(t) = V \quad \text{for } |t| \leq T/2$$

$$= 0 \quad \text{for } T/2 < |t| < (\tau - T/2)$$

with $V(t + \tau) = V(t)$. The Fourier series representation of this function is

$$V(t) \sim \frac{1}{2} A_o + \sum_{n=1}^{\infty} (A_n \cos n\omega t + b_n \sin n\omega t)$$

where $\omega = 2\pi/\tau$ and

$$A_o = \frac{2}{\tau} \int_{-\tau/2}^{\tau/2} V(t)\, dt = 2\,\frac{VT}{\tau}$$

$$A_n = \frac{2}{\tau} \int_{-\tau/2}^{\tau/2} V(t) \cos n\omega t\, dt = \frac{2V}{n\pi} \sin \frac{n\pi T}{\tau}$$

$$b_n = \frac{2}{\tau} \int_{-\tau/2}^{\tau/2} V(t) \sin n\omega t\, dt = 0$$

Hence

$$V(t) \sim \frac{VT}{\tau} + \sum_{n=1}^{\infty} \frac{2V}{n\pi} \sin \pi T f_n \cos \omega_n t$$

where $\omega_n = n\omega = 2\pi f_n$. The spectral distribution therefore consists of discrete frequency components at $f_n = n/\tau$ whose amplitude variations have the pattern of a sinc function with zeros at f = 1/T, 2/T, ... The function V(t) and its spectral distribution are plotted in Figure 19 for T = 0.6 ns and τ = 15 ms. The spectral distribution throughout the FM broadcast band is flat to within less than 0.5%.

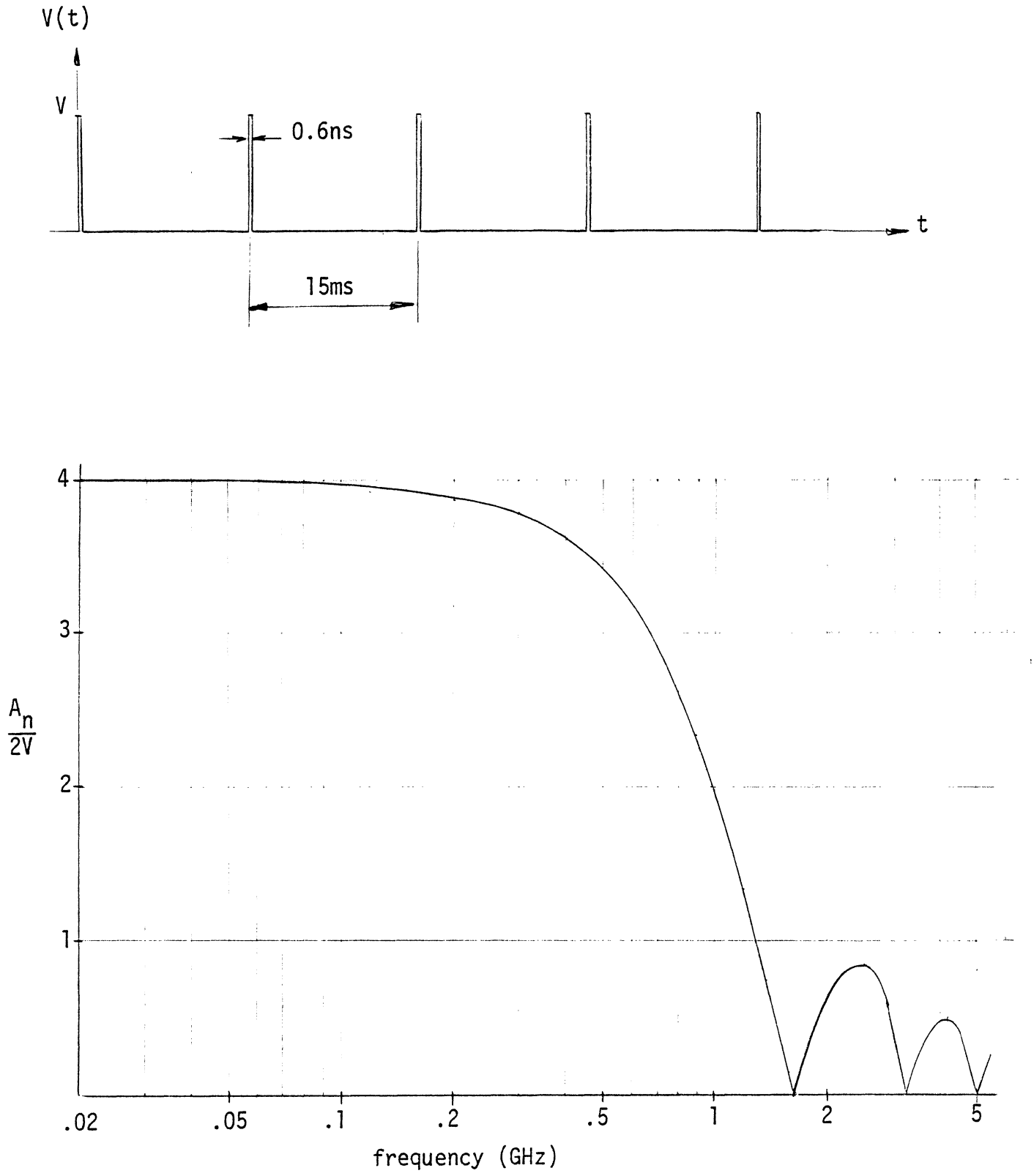

Figure 19. Spectral distribution of simulated ignition radiation

APPENDIX B:

COMPUTATION OF THE SPECTRAL DISTRIBUTION OF IGNITION NOISE

The representation of ignition noise shown in Figure 12 is described by the periodic function

$$V(t) = \frac{V_1}{t_1} t \qquad 0 \leq t \leq t_1$$

$$= V_1 + \frac{V_2 - V_1}{t_2 - t_1} (t - t_1) \qquad t_1 \leq t \leq t_2$$

$$= V_2 - \frac{V_2}{t_3 - t_2} (t - t_2) \qquad t_2 \leq t \leq t_3$$

$$= 0 \qquad t_3 \leq t \leq \tau$$

with $V(t + \tau) = V(t)$. Expanding $V(t)$ in a Fourier series

$$V(t) \sim \frac{1}{2} A_o + \sum_{n=1}^{\infty} (A_n \cos n\omega t + b_n \sin n\omega t) \tag{1}$$

where $\omega = 2\pi/\tau$ and

$$A_n = \frac{2}{\tau} \int_o^{\tau} V(t) \cos n\omega t \, dt$$

$$b_n = \frac{2}{\tau} \int_o^{\tau} V(t) \sin n\omega t \, dt$$

the Fourier coefficients can be expressed as

$$A_n = \frac{2}{\tau} \sum_{i=1}^{5} \alpha_i A_{ni} \qquad b_n = \frac{2}{\tau} \sum_{i=1}^{5} \alpha_i b_{ni} \tag{2}$$

where

$$\alpha_1 = \frac{V_1}{t_1} \qquad \alpha_4 = V_2 + \frac{V_2}{t_3 - t_2} t_2$$

$$\alpha_2 = V_1 - \frac{V_2 - V_1}{t_2 - t_1} t_1 \qquad \alpha_5 = \frac{-V_2}{t_3 - t_2}$$

$$\alpha_3 = \frac{V_2 - V_1}{t_2 - t_1}$$

and the terms A_{ni} and b_{ni} are given by

$$A_{n1} = \int_0^{t_1} t \cos n\omega t \, dt \qquad b_{n1} = \int_0^{t_1} t \sin n\omega t \, dt$$

$$A_{n2} = \int_{t_1}^{t_2} \cos n\omega t \, dt \qquad b_{n2} = \int_{t_1}^{t_2} \sin n\omega t \, dt$$

$$A_{n3} = \int_{t_1}^{t_2} t \cos n\omega t \, dt \qquad b_{n3} = \int_{t_1}^{t_2} t \sin n\omega t \, dt$$

$$A_{n4} = \int_{t_2}^{t_3} \cos n\omega t \, dt \qquad b_{n4} = \int_{t_2}^{t_3} \sin n\omega t \, dt$$

$$A_{n5} = \int_{t_2}^{t_3} t \cos n\omega t \, dt \qquad b_{n5} = \int_{t_2}^{t_3} t \sin n\omega t \, dt$$

For n = 0:

$$A_{01} = \frac{(t_1)^2}{2} \qquad A_{04} = t_3 - t_2$$

$$A_{02} = t_2 - t_1 \qquad A_{05} = \frac{(t_3)^2 - (t_2)^2}{2}$$

$$A_{03} = \frac{(t_2)^2 - (t_1)^2}{2}$$

For $n \geq 1$:

$$A_{n1} = \left(\frac{\tau}{2\pi n}\right)^2 \left(\cos \frac{2\pi n t_1}{\tau} - 1\right) + \frac{t_1 \tau}{2\pi n} \sin \frac{2\pi n t_1}{\tau}$$

$$A_{n2} = \frac{\tau}{2\pi n} \left(\sin \frac{2\pi n t_2}{\tau} - \sin \frac{2\pi n t_1}{\tau}\right)$$

$$A_{n3} = \left(\frac{\tau}{2\pi n}\right)^2 \left(\cos \frac{2\pi n t_2}{\tau} - \cos \frac{2\pi n t_1}{\tau}\right) + \frac{\tau}{2\pi n} \left(t_2 \sin \frac{2\pi n t_2}{\tau} - t_1 \sin \frac{2\pi n t_1}{\tau}\right)$$

$$A_{n4} = \frac{\tau}{2\pi n} \left(\sin \frac{2\pi n t_3}{\tau} - \sin \frac{2\pi n t_2}{\tau}\right)$$

$$A_{n5} = \left(\frac{\tau}{2\pi n}\right)^2 \left(\cos \frac{2\pi n t_3}{\tau} - \cos \frac{2\pi n t_2}{\tau}\right) + \frac{\tau}{2\pi n} \left(t_3 \sin \frac{2\pi n t_3}{\tau} - t_2 \sin \frac{2\pi n t_2}{\tau}\right)$$

$$b_{n1} = \left(\frac{\tau}{2\pi n}\right)^2 \sin \frac{2\pi n t_1}{\tau} - \frac{t_1 \tau}{2\pi n} \cos \frac{2\pi n t_1}{\tau}$$

$$b_{n2} = \frac{\tau}{2\pi n} \left(\cos \frac{2\pi n t_1}{\tau} - \cos \frac{2\pi n t_2}{\tau}\right)$$

$$b_{n3} = \left(\frac{\tau}{2\pi n}\right)^2 \left(\sin \frac{2\pi n t_2}{\tau} - \sin \frac{2\pi n t_1}{\tau}\right) + \frac{\tau}{2\pi n} \left(t_1 \cos \frac{2\pi n t_1}{\tau} - t_2 \cos \frac{2\pi n t_2}{\tau}\right)$$

$$b_{n4} = \frac{\tau}{2\pi n} \left(\cos \frac{2\pi n t_2}{\tau} - \cos \frac{2\pi n t_3}{\tau}\right)$$

$$b_{n5} = \left(\frac{\tau}{2\pi n}\right)^2 \left(\sin \frac{2\pi n t_3}{\tau} - \sin \frac{2\pi n t_2}{\tau}\right) + \frac{\tau}{2\pi n} \left(t_2 \cos \frac{2\pi n t_2}{\tau} - t_3 \cos \frac{2\pi n t_3}{\tau}\right)$$

Substituting these results into (2) yields

$$A_0 = \frac{1}{\tau} \left\{V_1 t_2 + V_2 (t_3 - t_1)\right\}$$

$$A_n = \frac{\tau}{2n^2\pi^2} \left\{\frac{-V_1}{t_1} + \left(\frac{V_1}{t_1} - \frac{V_2 - V_1}{t_2 - t_1}\right) \cos \frac{2\pi n t_1}{\tau} + \left(\frac{V_2 - V_1}{t_2 - t_1} + \frac{V_2}{t_3 - t_2}\right) \cos \frac{2\pi n t_2}{\tau} - \frac{V_2}{t_3 - t_2} \cos \frac{2\pi n t_3}{\tau}\right\}$$

$$b_n = \frac{\tau}{2n^2\pi^2}\left\{\left(\frac{V_1}{t_1} - \frac{V_2 - V_1}{t_2 - t_1}\right)\sin\frac{2\pi n t_1}{\tau} + \left(\frac{V_2 - V_1}{t_2 - t_3} + \frac{V_2}{t_3 - t_2}\right)\sin\frac{2\pi n t_2}{\tau} - \frac{V_2}{t_3 - t_2}\sin\frac{2\pi n t_3}{\tau}\right\}$$

These expressions are now in a suitable form to enable computation of the Fourier series (1). However, the spectrum analyzer used in the analysis of the audio noise measures the RMS value of the voltage in decibels above one volt. For comparison it is therefore necessary to compute the RMS value of each frequency component of the series and express the result in dBV. At the frequency $f_n = n/\tau$, the RMS voltage, in millivolts, is

$$V_{RMS}^2 = \frac{n}{\tau}\int_0^{\tau/n} (A_n \cos n\omega t + b_n \sin n\omega t)^2\, dt = \frac{(A_n)^2}{2} + \frac{(b_n)^2}{2}$$

Expressing the result in dBV yields

$$V_{RMS} = 10 \log\left(\frac{(A_n)^2 + (b_n)^2}{2}\right) - 60 \qquad \text{dVB.}$$